CHEMISTRY
A European Journal

A Journal of
ChemPubSoc Europe

Accepted Article

Title: Calcium-Responsive Liposomes via a Synthetic Lipid Switch

Authors: Jinchao Lou, Adam Carr, Alexa Watson, Samuel Mattern-Schain, and Michael D Best

To be cited as: *Chem. Eur. J.* 10.1002/chem.201705810

Link to VoR: http://dx.doi.org/10.1002/chem.201705810

Supported by
ACES

WILEY-VCH

10.1002/chem.201705810

WILEY-VCH

Calcium-Responsive Liposomes via a Synthetic Lipid Switch

Jinchao Lou, Adam J. Carr, Alexa J. Watson, Samuel I. Mattern-Schain and Michael D. Best*[a]

This article is dedicated to the memory of Tracy Kolb Osborne.

Abstract: Liposomal drug delivery would benefit from enhanced control over content release. Here, we report a novel avenue for triggering release driven by chemical composition using liposomes sensitized to calcium, a target chosen due to its key roles in biology and disease. To demonstrate this principle, we synthesized calcium responsive lipid switch **1**, designed to undergo conformational changes upon calcium binding that perturb membrane integrity, thereby promoting release. This was shown through fluorescence-based release assays via dose-dependent response depending on the percentage of **1** in liposomes, with minimal background leakage in controls. DLS experiments indicated dramatic changes in particle sizes upon treatment of liposomes containing **1** with calcium. In a comparison of ten naturally occurring metal cations, calcium provided the greatest release. Finally, STEM images showed significant changes in liposome morphology upon treatment of liposomes containing **1** with calcium. These results showcase lipid switches driven by molecular recognition principles as an exciting avenue for controlling membrane properties.

Introduction

Liposomes are effective supramolecular nanocarriers for drug delivery and imaging applications due to their ability to encapsulate and deliver a range of molecular cargo with varying properties. Indeed, liposome formulations have been clinically approved for the delivery of drugs that possess poor pharmacokinetic properties on their own.[1] Despite this demonstrated efficacy, challenges remain in the optimization of drug delivery characteristics. In particular, the ability to control the release of therapeutic or diagnostic contents to achieve selective delivery within targeted diseased cells is a key aspect to maximize encapsulated drug efficacy while minimizing off-target effects. As a result, a variety of approaches for triggering release from liposomes have been investigated, which have commonly utilized either pathophysiological conditions (passive release) or external stimuli (active release) to drive drug release.[2] For passive release, characteristics of diseased cells including acidity,[3] reducing environments,[4] and aberrant enzyme expression[5] have been exploited to stimulate liposomal release. Regarding external stimuli, light-initiated release using photocleavable moieties,[6] ultrasound-mediated leakage,[7] and liposome disruption through heat[8] have been reported.

While these approaches have proven to be successful in vitro, many challenges remain for maximizing controlled release in real-world drug delivery applications. Diseased cells possess different properties that can be targeted through passive release mechanisms. However, these conditions often show minimal variation from normal cells. For example, the average extracellular pH of cancer cells has been measured as 6.5–6.9 compared to 7.2–7.4 for normal tissue, providing a narrow window for differentiation.[9] Approaches involving external stimuli on the other hand suffer from the challenges associated with delivering stimuli to a defined target location in a non-destructive manner. For example, while photocleavable liposomes have been extensively studied, release from these systems typically results from irradiation with UV light, which suffers from minimal penetration of tissue and the photodecomposition of many biological molecules that absorb in this range of the electromagnetic spectrum.

Herein, we describe an alternative approach for selective liposome disruption by triggering release based on the chemical/metabolic profiles of diseased cells. This provides a promising means for differentiating between healthy and diseased cells, which generally have significantly different chemical compositions. Our initial approach involves the release of encapsulated contents from liposomes driven by calcium binding. Calcium was selected as a critical biological cation that regulates cell death,[10] muscle contraction,[11] neuronal transduction,[12] immune responses[13] and numerous intra- and extracellular signaling pathways.[14] Human serum concentrations of calcium are in the low millimolar range,[14-15] while cytosolic amounts are lower (~100 nM) since calcium is pumped out of this region.[16] Some cytosolic calcium is pumped into the endoplasmic reticulum (ER), which maintains higher calcium concentrations (~1 mM), as do mitochondria.[17] Calcium overload, particularly in the ER, has been linked to diseases[18] including Alzheimer's disease,[19] amyotrophic lateral sclerosis (ALS),[20] Gaucher's disease[21] and ischemic stroke.[22] Calcium abundance is a critical aspect associated with malaria,[23] in which *Plasmodium* parasites are reliant upon ~30 calcium-responsive metalloproteins.[17, 24] Thus, calcium is required for cell invasion and egress,[25] and calcium concentration increases to 10-20 fold in invaded cells above normal concentrations.[26] Molecules that diminish free calcium such as chelating ligands inhibit parasite invasion.[25, 27] Finally, calcium regulates aspects of cancer physiology,[28] and is found in greater abundance in certain metastasizing cancer cells.[29] For these reasons, calcium provides an exciting target for triggering release of liposomal therapeutics.

[a] J. Lou, A.J. Carr, A.J. Watson, S.I. Mattern-Schain, Prof. M.D. Best
Department of Chemistry, University of Tennessee
1420 Circle Drive, Knoxville, TN 37996 (USA)
E-mail: mdbest@utk.edu

Supporting information for this article is given via a link at the end of the document.

Results and Discussion

The work reported here was inspired by previous efforts in liposome release, such as acid-responsive lipids. For example, Leblond and co-workers reported a bis-(methoxyphenyl)pyridine system in which protonation of the central pyridine nitrogen leads to rotation of methoxyphenyl groups to promote hydrogen bonding, thereby disrupting the membrane and triggering release.[30] Additionally, Menger and co-workers reported a morpholinocyclohexanol- (MOCH)-lipid that undergoes a cyclohexanol chair flip upon morpholine protonation to help trigger release when the liposomes are tethered to spherical polycationic brushes.[3g] Regarding release driven by binding interactions, Smith and co-workers utilized a sensor that targets the lipid phosphatidylserine (PS) to trigger release from liposomes containing PS.[31] This last example demonstrates that a non-covalent binding event can drive membrane disruption and release. Our work seeks to build upon this principle by incorporating the sensor motif into the lipid structure so as to engineer liposomes to undergo conformational changes that perturb bilayer packing and trigger release upon recognition.

The design of a calcium-responsive lipid switch also benefits from the availability of known sensors that exhibit affinity and selectivity calcium ions. One such example is the fluorescent sensor indo-1, which has been widely utilized for the detection of calcium in biological systems.[32] Indo-1 binds to calcium with a K_d of 250 nM, and exhibits selectivity in the presence of millimolar concentrations of magnesium.[32a] In the design of calcium-responsive lipid **1**, hydrophobic lipid chains were grafted onto the calcium recognition domain. It was envisaged that these chains would rest comfortably within the membrane bilayer when the binding groups are present in an open form, and that calcium binding (**1-Ca**) would lead to constriction of the chelating groups, thereby forcing the chains to move in opposite directions. This conformational change was expected to result in a dramatically increased cone angle in lipid **1-Ca**, thereby mimicking the properties of non-bilayer lipids,[33] which create pressure and defects within the membrane. In this way, the system was designed to perturb the organization of the membrane bilayer upon calcium

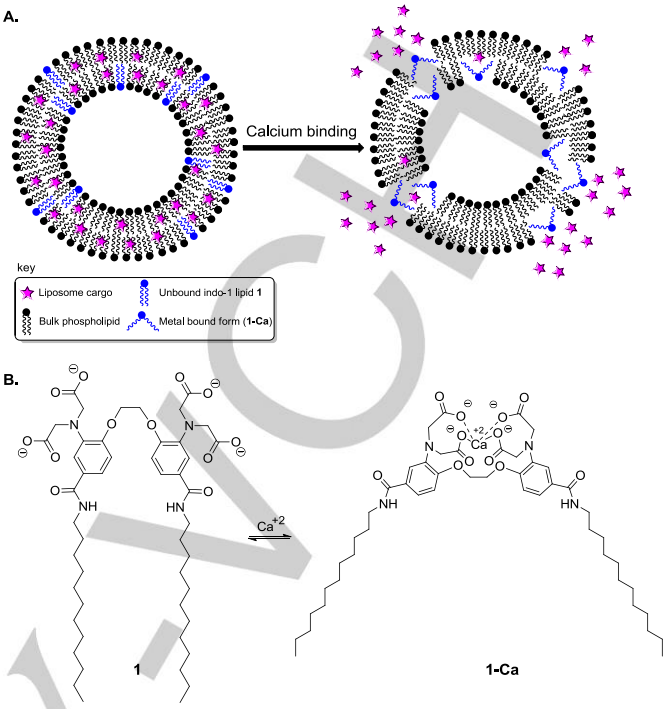

Scheme 1. Calcium-triggered liposomal release. **A.** Cartoon for liposome release driven by membrane perturbation upon calcium binding. **B.** Hypothetical conformational changes of lipid switch **1** upon calcium binding to form **1-Ca**.

binding and thereby trigger release of contents as shown in Scheme 1.

The synthesis of **1**, which benefitted from the prior synthesis of indo-1,[32a] is shown in Scheme 2. This commenced with 4-hydroxy-3-nitrobenzoic acid (**2**), which was coupled to dodecylamine to introduce the hydrophobic lipid chains through the amide linkage of **3**. Two equivalents of this product were then reacted with dibromoethane to generate **4**. Next, the nitro groups of this intermediate were reduced to the amine groups of **5a**, followed by alkylation with four equivalents of bromoethylacetate to produce **5b**. Finally, ester hydrolysis generated lipid switch **1**. Following the synthesis, we set out to evaluate triggered release from liposomes incorporating **1** by conducting fluorescence

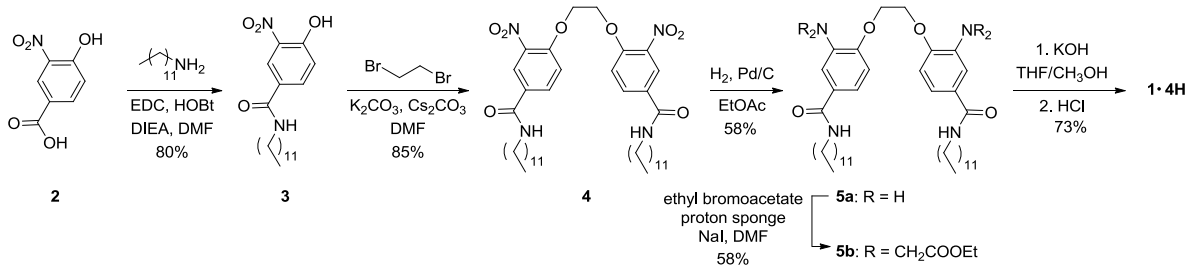

Scheme 1. Synthesis of calcium-responsive lipid switch **1**. A dodecylamine group was coupled onto precursor **2** to produce the amide of **3**, followed by dimerization through reaction of the phenol group with dibromoethane to **4**, nitro reduction to the amines of **5a**, alkylation to introduce four ethylacetate groups to access **5b**, and finally ester hydrolysis to generate **1** in its protonated form.

10.1002/chem.201705810

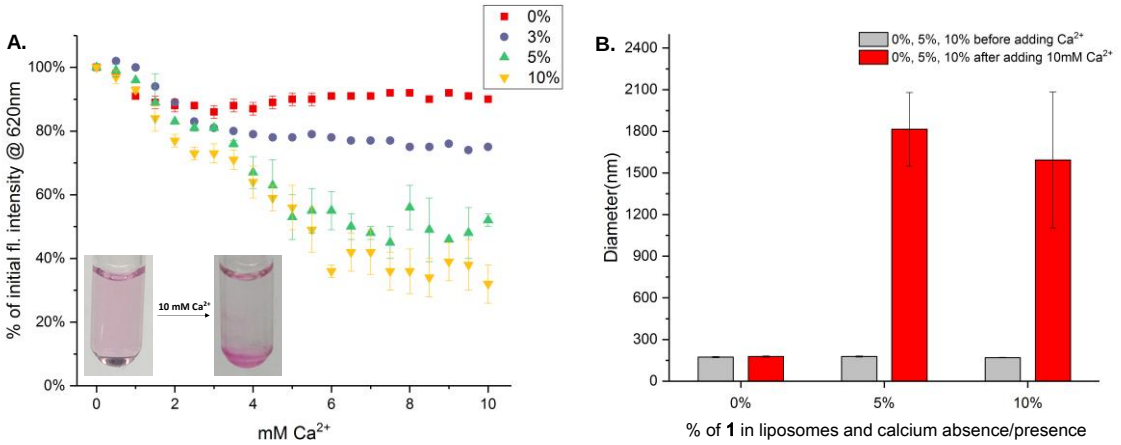

Figure 1. Results from fluorescence nile red release experiments and DLS studies using liposomes containing **1**. A. Dose-dependent release of nile red from PC liposomes containing 0%, 3%, 5%, and 10% of lipid **1**. Inset shows images before and after release of liposomes containing 10% of **1** with 10 mM calcium. B. DLS results before and after calcium addition indicate initial stable liposomes that undergo dramatic changes in size only when lipid **1** is present. All data represent the averages of at least three replicates with error bars indicating standard errors.

release assays employing the dye nile red. Nile red is a hydrophobic fluorophore that is solubilized by encapsulation within liposome bilayers, and therefore mimics the properties of commonly used non-polar drugs.[34] This leads to a standard fluorescence signal for the dye when solubilized by the liposomes. Upon leakage of nile red from the liposomes, this compound is rendered insoluble. Thus, release can be tracked by the reduction in fluorescence of the sample.

In studies, we prepared liposomes that were primarily composed of PC (mixed isomers) and doped with 0% (control), 3%, 5% or 10% of lipid **1**. Standard thin-film hydration procedures were used to prepare unilamellar liposomes from chloroform solutions containing the desired lipid mixtures via drying, hydration, freeze/thaw cycling, and extrusion through 200 nm filters. Incorporation of **1** within resulting liposomes was confirmed by UV/Vis experiments performed before and after formation (see supplementary information for details).

After an initial fluorescence scan, each liposome sample was titrated with calcium chloride to a final concentration of 10 mM. As can be seen from the results shown in Figure 1A, we observed a gradual decrease in nile red fluorescence upon titration with calcium that was dependent on the percentage of **1** in liposomes. Results from control liposomes lacking **1** indicated a background fluorescence decrease of ~10%, which is in line with previous work.[34] This was enhanced to ~25% decrease with liposomes containing 3% of **1**, ~50% with 5% of **1**, and ~65% with 10% of **1**. These results show that the extent of release correlates with the percentage of lipid **1**, validating that our switchable lipid causes release of bilayer cargo. The effects of dilution in the titration were accounted for by subtracting out the minor decreases in fluorescence caused by diluting liposomes with water rather than treating with calcium. It should be noted that the percentage fluorescence change may not indicate the full amount of dye leakage since the released dye may re-enter liposomes or other reorganized lipid assemblies after initial release. These experiments were also performed in buffered solutions, in which release was diminished somewhat, as would be expected due to competition for calcium binding by the buffer. For example, while liposomes containing 10% of **1** yielded an ~65% fluorescence decrease following calcium titration in water, this was diminished to an ~25% drop in 1mM HEPES buffer at pH 7.4 (data not shown). While controlling release in vivo is challenging due to the presence of cation-binding competitors, these results indicate that calcium-triggered release can be accomplished in concentrated solutions.

Next, dynamic Light Scattering (DLS) experiments were performed to probe for changes in liposome structure upon treatment with calcium. Here, PC liposomes doped with 0% (control), 5%, and 10% of **1** were evaluated for particle size before and after calcium treatment. As seen in Figure 1B, the initial measurement for all three of these samples yielded similar average sizes, supporting that stable liposomes can be formed consisting of PC and lipid **1** up to at least 10%. Upon treatment with 10 mM calcium, control samples showed no change, while liposomes containing 5% and 10% of **1** each underwent a dramatic increase in size. This is consistent with changes in membrane properties such as reorganization into different lipid assemblies or membrane fusion. These results support the fluorescence release assays and provide evidence of physical changes in membrane properties driven by calcium binding only when lipid switch **1** is part of the liposomal architecture.

We next moved to assess the selectivity of the release system for calcium over other metal cations that are present in biological systems, including zinc, magnesium, nickel, cobalt, iron, sodium, potassium, copper and manganese. Release was evaluated by subjecting nile red encapsulating liposomes containing 10% of **1** to the appropriate chloride salts of the metal under investigation at a final concentration of 10 mM. Figure 2 shows the relative

fluorescence signal in the presence of each salt solution compared to the initial fluorescence of the nile red liposomes in water. Here, calcium yielded the greatest decrease in signal. Incubation with the monovalent cations sodium and potassium led to virtually no change, as was the case with divalent zinc. The other salt solutions tested resulted in intermediate release, which is line with the known challenges associated with differentiating between these metal cations.[32a] However, these competitors are present in low abundance in nature and commonly restricted to protein-bound forms. These results demonstrate that switchable lipid **1** exhibits enhanced release upon treatment with calcium, particularly when compared to the more abundant cations that exist in unbound forms in nature.

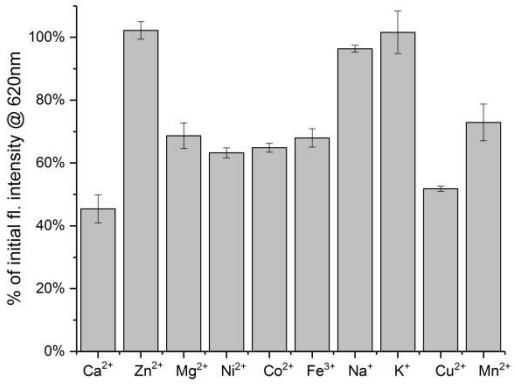

Figure 2. Comparison of nile red release using different naturally occurring metals. Zinc, sodium and potassium resulted in minimal release. Calcium yielded the greatest release, although other transition metals provided intermediate release.

A beneficial attribute of liposomes is that they can encapsulate both hydrophobic cargo within the membrane bilayer and hydrophilic agents in the aqueous core. The ability to deliver and release hydrophilic molecules is also of significant interest for the delivery of polar agents such as nucleic acids for gene therapy. The release of such agents is typically more challenging as it requires that polar/charged molecules traverse the membrane to ultimately escape liposomes. Thus, significant disruption of the membrane must be achieved to promote the leakage of polar molecules. We next moved to gauge the release of contents from the aqueous interiors of liposomes using a sulforhodamine B dye release assay. In these experiments, the dye is encapsulated within liposome aqueous interiors at high concentrations such that fluorescence is quenched by collisional effects. Since the dye is non-specifically encapsulated during liposome formation, size exclusion chromatography must be performed to separate liposomes from unencapsulated dye. Upon release from the liposome, the dye diffuses into bulk solvent and is diluted, thereby activating fluorescence.

To assess release from our calcium-responsive system, we encapsulated sulforhodamine B within liposomes containing 10% of **1** and 90% PC as well as control liposomes formed entirely from PC and again titrated with calcium. At the end of each titration, liposomes were treated with the detergent Triton X-100 to release all contents. To normalize the results in Figure 3, the extent of fluorescence increase is plotted as a percentage of each liposome's maximum fluorescence following Triton X-100 treatment. As can be seen from these results, liposomes containing **1** exhibit greater increases in fluorescence attributable to dye release compared to control liposomes. These results indicate that the calcium-responsive liposomes can release polar agents upon calcium treatment.

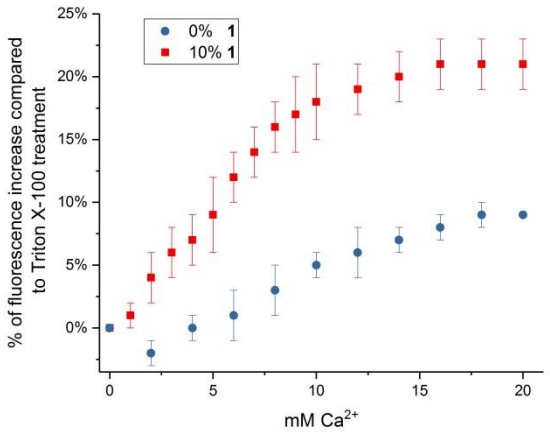

Figure 3. Increase in sulforhodamine B fluorescence upon calcium titration relative to maximum fluorescence upon Triton X-100 addition. Liposomes containing 10% of lipid **1** yielded a greater increase in fluorescence, attributable to dye release, compared to PC liposomes. Error bars indicate standard errors from at least three studies.

Finally, to probe for calcium-driven changes in liposome integrity, we performed scanning transmission electron microscopy (STEM) experiments to obtain images of the liposomes. This was performed using liposomes containing 10% of **1** before and after treatment with 20 mM calcium. As can be seen from the images shown in Figure 4, both the liposomes containing 10% of **1** before calcium addition (A) and the liposomes containing entirely PC after calcium addition (B) show comparable images of unilamellar liposomes with defined membranes of the expected sizes. The liposomes appear to be aggregated in these images, which may occur when liposomes are immobilized on carbon grids for STEM imaging, and thus may not be reflective of behavior in solution. Indeed, the DLS results shown in Figure 1B indicate that the liposomes are not aggregating into larger assemblies when free in solution. The images that were obtained from the liposome samples containing 10% of **1** after treatment with calcium (C) show

substantial changes to lipid morphology. Here, we observed complicated multilamellar or multivesicular assemblies driven by the calcium addition. Amorphic lipid assemblies with areas of extreme blebbing are observed in C, while such vesicles are not visible in A or B. Larger images are included in the supplementary information section.

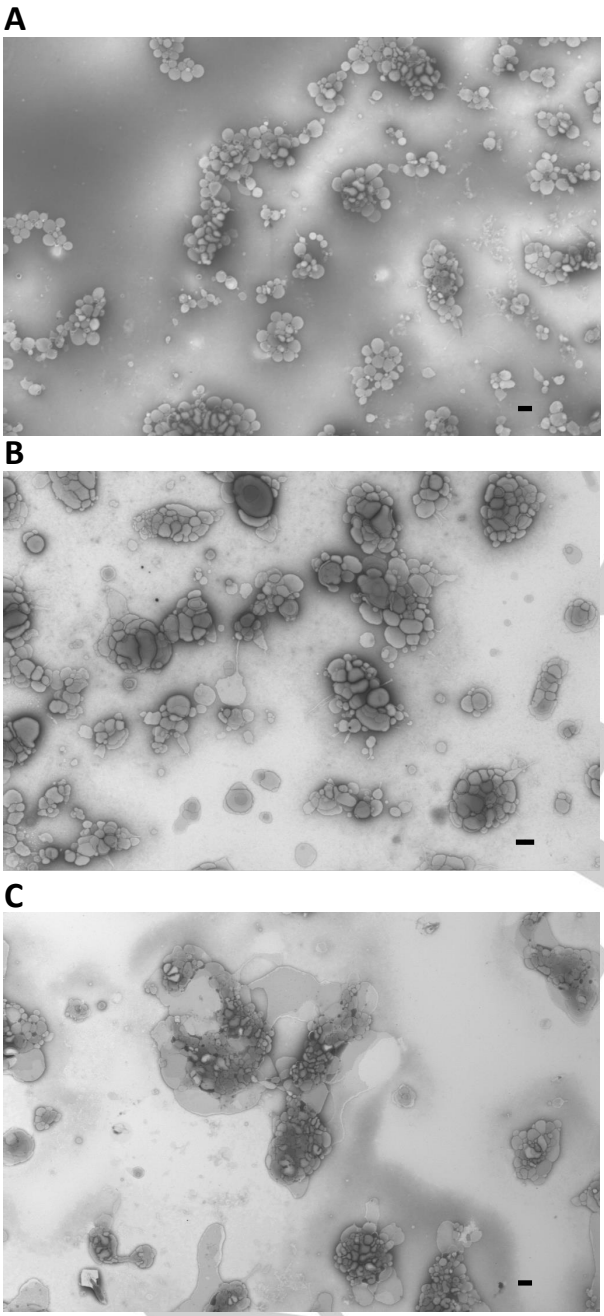

Figure 4. STEM images of liposomes (A) containing 10% of **1** before calcium addition, (B) containing 0% of **1** after 20 mM calcium addition, and (C) containing 10% of **1** after 20 mM calcium addition. The scale bar in each image denotes 200 nm.

Alternate explanations for content release in this system driven by calcium include liposome aggregation, fusion or lipid reorganization. Previously, vesicle fusion upon calcium addition has been observed in membranes containing high percentages or completely composed of anionic lipids such as phosphatidylserine (PS).[35] In these cases, calcium is believed to act as a bridging cation that connects lipid molecules from separate vesicles. In the current system, the tetraacetate groups of **1** are expected to fully encapsulate calcium ions. Indeed, the STEM results showing complex assemblies of diminished size could be explained by the perturbation of membrane properties in a manner that drives lipid reorganization. One note is that the significant changes in membrane architecture we observed may prove challenging for cases in which gradual controlled release is desired. However, the STEM images indicate the initial state and final form after treatment with 20 mM calcium, and thus do not provide insights into intermediate states during titrations.

Conclusions

Calcium-responsive lipid switch **1** opens a new paradigm for controlling the release of therapeutic cargo from liposomes driven by the molecular environment of cells and tissues. This is an exciting new avenue since it is often the abundance of metabolites that exhibits the greatest variation between normal and diseased cells. Thus, calcium-driven release can be probed as an effective means for selective delivery and release in and around diseased cells, such as those infected with the *Plasmodium* associated with malaria. In addition, many other biomolecules that are aberrantly expressed in disease could prove to be promising additional promising targets for the development of additional membrane release systems driven by lipid switches.

Experimental Section

General Experimental

Reagents and solvents were generally purchased from Acros, Aldrich, or Fisher Scientific and used without further purification. PC (L-α-phosphatidylcholine, mixed isomers from chicken eggs) was purchased from Avanti Polar Lipids, Inc. Dry solvents were obtained from a Pure solvent delivery system purchased from Innovative Technology, Inc. Column chromatography was performed using 230−400 mesh silica gel purchased from Sorbent Technologies. NMR spectra were obtained using Varian 500 MHz spectrometer. Mass spectra were obtained with JEOL DART-AccuTOF and Q-Star XL quadrupole time-of-flight hybrid mass spectrometer (Applied Biosystems, Foster City, CA). Liposome extruder and polycarbonate membranes were obtained from Avestin (Ottawa, Canada). Ultrapure water was purified via a Millipore water system (≥18 MΩ·cm triple water purification system). Small quantities (<5 mg) were weighed on a OHRUS analytical-grade mass balance. Fluorescence studies were performed using a PerkinElmer LS55 fluorimeter. Plots were generated using Origin Pro 2017. All the error bars showed the standard errors of at least three experimental replicates.

N-Dodecyl-4-hydroxy-3-nitrobenzamide (3)

4-hydroxy-3-nitrobenzoic acid (**2**, 1g, 5.46mmol), dodecan-1-amine (1.52g, 8.2mmol) and hydroxybenzotriazole (HOBt, 1.256g, 8.2mmol) were dissolved in 15 ml DMF under argon atmosphere. After being cooled to 0 °C and stirred for 5 minutes, 1-(3-dimethylaminopropyl)-3-ethylcarbodiimide hydrochloride (EDCI•HCl, 1.57g, 8.2mmol) and N, N-

diisopropylethylamine (DIEA, 2.4ml, 13.65 mmol) were added. The reaction mixture was opaque orange. Then, the ice bath was removed and the reaction mixture was further stirred at room temperature for 5 hours. The reaction was quenched by adding 3 ml water and poured into 1M HCl. Ethyl acetate was then added to the mixture and the organic phase was washed five times with water and twice with brine. After the removal of the organic solvent under reduced pressure, the crude product was recrystallized with 95% ethanol to afford compound **3** as a pale yellow solid (1.54g, 4.39 mmol, 80% yield). ^{1}H NMR (500 MHz, $CDCl_3$) δ 10.76 (s, 1H), 8.50 (d, *J* = 2.2 Hz, 1H), 8.06 (dd, *J* = 8.8, 2.3 Hz, 1H), 7.23 (d, *J* = 8.7 Hz, 1H), 6.11 (s, 1H), 3.45 (td, *J* = 7.3, 5.7 Hz, 2H), 1.63 (ddd, *J* = 14.8, 8.1, 6.7 Hz, 2H), 1.39 – 1.24 (m, 18H), 0.92 – 0.85 (m, 3H); ^{13}C NMR (126 MHz, $CDCl_3$) δ 164.57, 157.03, 136.09, 127.23, 123.65, 120.48, 40.40, 31.92, 29.65, 29.63, 29.59, 29.54, 29.35, 29.32, 27.00, 22.69, 14.12; HRMS-DART: $[M+H]^+$ calcd for $C_{19}H_{31}N_2O_4$, 351.2283, found 351.2252.

4,4'-(Ethane-1,2-diylbis(oxy))bis(*N*-dodecyl-3-nitrobenzamide (4)
In a round bottom flask, compound **3** (1.0381g, 2.96 mmol) was combined with oven-dried Cs_2CO_3 (1.265g, 3.88 mmol) and K_2CO_3 (0.691g, 5 mmol) under nitrogen. Then, 15ml DMF was added and followed by 1,2-dibromoethane (0.1276 ml, 1.48 mmol). After refluxing for 24 hours, the reaction mixture was cooled down to room temperature first. Enough water was added to obtain yellow suspension and then the suspension was extracted twice by chloroform (determined by TLC). The organic phases were collected and then washed three times by water, once with brine, dried with Na_2SO_4, filtered and concentrated under reduced pressure. Column chromatography using gradient elution from 50% ethyl acetate-hexane to 10% methanol-dichloromethane afforded pale yellow compound **4** (0.9189g, 1.264 mmol, 85% yield). Rf=0.5 (5% methanol-ethyl acetate), ^{1}H NMR (500 MHz, $CDCl_3$) δ 8.20 (d, *J* = 2.3 Hz, 2H), 8.02 (dd, *J* = 8.7, 2.3 Hz, 2H), 7.28 (s, 1H), 7.26 (d, *J* = 0.4 Hz, 1H), 6.10 (t, *J* = 5.7 Hz, 2H), 4.61 (s, 4H), 3.45 (td, *J* = 7.3, 5.6 Hz, 4H), 1.66 – 1.59 (m, 4H), 1.42 – 1.24 (m, 36H), 0.90 – 0.85 (m, 6H). ^{13}C NMR (126 MHz, $CDCl_3$) δ 164.79, 153.90, 139.77, 133.15, 128.38, 124.43, 115.61, 68.86, 40.55, 32.07, 29.80, 29.78, 29.75, 29.69, 29.50, 29.46, 27.15, 22.84, 14.28., HRMS-DART: $[M+H]^+$ calcd for $C_{40}H_{63}N_4O_8$, 727.4646, found 727.4397.

4,4'-(Ethane-1,2-diylbis(oxy))bis(3-amino-*N*-dodecylbenzamide) (5a)
Compound **4** (0.2431g, 0.334mmol) and 10% Pd/C (0.0486g, 20% weight of compound **4**) were added to a round bottom flask and dissolved in 20 ml ethyl acetate under argon. Then, argon was replaced by hydrogen atmosphere and the reaction mixture was further stirred under H_2 at room temperature for 12 hours. The Pd/C was carefully removed via a celite pad. After the removal of solvent under reduced pressure, the crude product was purified with column chromatography packed with alumina using eluent of 100% chloroform to 1% methanol-chloroform to afford compound **5** (130mg, 0.195mmol, 58%) as light yellow solid. R_f = 0.4 (7.5% methanol-chloroform), ^{1}H NMR (500 MHz, $CDCl_3$) δ 7.10 (d, *J* = 2.2 Hz, 2H), 7.05 (dd, *J* = 8.4, 2.2 Hz, 2H), 6.79 (d, *J* = 8.4 Hz, 2H), 6.55 (t, *J* = 5.7 Hz, 2H), 4.37 (s, 4H), 3.32 – 3.24 (m, 8H), 1.60 – 1.46 (m, 4H), 1.34 – 1.07 (m, 36H), 0.86 – 0.75 (m, 8H). ^{13}C NMR (126 MHz, $CDCl_3$) δ 167.42, 159.87, 153.89, 133.16, 124.44, 115.58, 111.39, 67.33, 40.56, 40.21, 32.07, 29.90, 29.86, 29.81, 29.78, 29.76, 29.72, 29.70, 29.50, 29.47, 27.19, 27.16, 22.85, 14.28. HRMS-DART: $[M+H]^+$ calcd for $C_{40}H_{66}N_4O_4$, 667.5162, found 667.4757.

Tetraethyl 2,2',2'',2'''-(((ethane-1,2-diylbis(oxy))bis(5-(dodecylcarbamoyl)-2,1-phenylene))bis(azanetriyl))tetraacetate (5b)
In a small vial, compound **5a** (40 mg, 0.06 mmol), sodium iodide (47.7 mg, 0.318 mmol) and proton sponge (68.13 mg, 0.318 mmol) were dissolved in 1ml DMF under argon. After addition of ethyl bromoacetate (53 μL, 0.318 mmol), the reaction mixture was stirred at 80 °C for 24 hours. After completion, DMF was removed under reduced pressure. The crude product was further purified by column chromatography using gradient elution of 100% chloroform to 6% methanol-chloroform and finally gave **5b** as a brown solid (35mg, 0.035mmol, 58% yield). R_f=0.3 (10% methanol-chloroform), ^{1}H NMR (500 MHz, $CDCl_3$) δ 7.32 (d, *J* = 2.2 Hz, 2H), 7.30 – 7.24 (m, 2H), 6.84 (d, *J* = 8.4 Hz, 2H), 6.03 (t, *J* = 5.7 Hz, 2H), 4.31 (s, 4H), 4.14 (s, 8H), 4.04 (q, *J* = 7.1 Hz, 8H), 3.41 (qd, *J* = 7.0, 2.9 Hz, 4H), 1.59 (qd, *J* = 8.6, 7.9, 4.5 Hz, 4H), 1.27 (d, *J* = 7.2 Hz, 36H), 1.16 (t, *J* = 7.2 Hz, 12H), 0.88 (t, *J* = 6.9 Hz, 6H); ^{13}C NMR (126 MHz, $CDCl_3$) δ 171.24, 166.95, 152.65, 139.41, 128.18, 120.63, 118.22, 112.32, 77.28, 77.03, 76.78, 67.17, 60.90, 53.50, 40.10, 31.92, 29.75, 29.66, 29.63, 29.61, 29.58, 29.56, 29.36, 29.35, 27.05, 27.03, 22.69, 14.18, 14.12, 14.07., HRMS-DART: $[M+H]^+$ calcd for $C_{56}H_{91}N_4O_{12}$, 1011.6634, found 1011.3491.

2,2',2'',2'''-(((Ethane-1,2-diylbis(oxy))bis(5-(dodecylcarbamoyl)-2,1-phenylene))bis(azanetriyl))tetraacetic acid (1•4H)
Compound **5b** (20mg, 0.0198mmol) was dissolved in 800 μL THF and 200 μL MeOH mixture in a vial. After adding 150 μL 1M KOH, the reaction mixture was stirred at room temperature overnight. After completion, the solvent was removed under reduced pressure. 5 ml water was then added to dissolve the crude product. Finally, 4M HCl was added dropwise. When the pH reached 1, precipitate came out. Vacuum filtration was used to obtain **1•4H** as pale brown solid (13mg, 0.014 mmol, 73% yield). ^{1}H NMR (500 MHz, 20% MeOD- $CDCl_3$) δ 7.35 – 7.29 (m, 2H), 7.27 (d, *J* = 2.0 Hz, 2H), 6.86 (dd, *J* = 8.3, 3.2 Hz, 2H), 4.29 (d, *J* = 3.1 Hz, 4H), 3.95 (d, *J* = 3.1 Hz, 8H), 3.34 – 3.23 (m, 4H), 1.52 (d, *J* = 8.2 Hz, 4H), 1.34 – 1.09 (m, 36H), 0.85 – 0.75 (m, 6H). ^{13}C NMR (126 MHz, 20% MeOD- $CDCl_3$) δ 174.25, 168.35, 153.14, 138.65, 128.17, 123.30, 118.16, 112.19, 77.80, 77.54, 77.28, 66.86, 55.20, 49.53, 49.36, 49.19, 49.02, 48.85, 48.68, 48.51, 40.46, 32.13, 29.88, 29.85, 29.82, 29.71, 29.62, 29.56, 27.30, 22.88, 14.17. ESI-MS: $[M-H]^+$ calcd for $C_{48}H_{73}N_4O_{12}$, 897.5225, found 897.4339.

Preparation of liposomes for nile red release studies
Lipid **1**, PC and nile red stock solutions were first prepared as follows: 5 mM nile red stock solution was prepared by dissolving 4.41 mg nile red in 2.77 mL chloroform, 32 mM PC stock solution was prepared by dissolving 25 mg PC with 1.014 mL chloroform, and for lipid **1** a 5 mM stock solution was prepared by dissolving 2.6 mg of **1** in 580 μL of50% methanol-chloroform. Next, proper volumes of each stock solution were pipetted into a clean vial to obtain the desired percentage of each component. As an example, to make 250 μL of a 2 mM liposome solution containing 10% of **1**, 13.3 μL PC (85%), 10 μL lipid **1** (10%) and 5 μL nile red (5%) were combined in a vial. The solvents were then evaporated under nitrogen stream and the resulting solid was further dried under vacuum for at least two hours to yield a lipid film. After that, the lipid film was hydrated with MilliQ purified water (250 μL) at 50 °C for 3 sets of 10 mins with vortexing after each set. 10 freeze-thaw cycles were done on the resulting liposome solution with dry/ice acetone bath and 50 °C water bath. Finally, the liposome solutions were extruded through a 200 nm polycarbonate membrane for 15 passes with a LiposoFast extruder (Avestin, Inc.). Other liposomes used for studies were produced in the same manner using different percentages of the lipid **1**.

Titrations of Liposomes Encapsulating Nile Red with Calcium Chloride Solutions
A 0.1 M Calcium chloride stock solution was made by dissolving calcium chloride into MilliQ purified water. A 100 μL aliquot of the 2 mM liposome solution prepared through the procedure above was added to a sub-micro quartz cuvette. The calcium chloride stock solution was added in 0.5 μL aliquots directly into the cuvette for each measurement in the titration (increment ~ 0.5 mM) and the fluorescence intensity was then measured (excitation wavelength = 552 nm, excitation slit = 10 nm, emission slit = 5 nm). Since dilution effect will also lower the fluorescence intensity, an additional control sample was run by instead adding 0.5 μL MilliQ water (no calcium) to a 100 μL solution of the same liposome. When processing the data, fluorescence intensities at 620 nm were selected and the intensity of the control sample was subtracted out to account for decreased signal resulting from dilution effect. Experiments were run at least 3 times each with different batches of liposomes, and averaged data were reported with error bars showing standard error.

Dynamic light scattering (DLS) Liposome Analysis During Calcium Addition
DLS measurements were carried out with a Malvern Zetasizer Nano ZS instrument equipped with a 4.0 mW laser operating at λ = 633 nm. Samples were prepared by diluting the liposome solutions before or after adding ions 10 times with MilliQ water. All samples were determined at a scattering angle of 173° at 25 °C. The data reported were the average of three tests with error bars showing standard error.

Metal Comparison Content Release Studies
0.1 M metal ion stock solutions were prepared by dissolving their chloride salts ($ZnCl_2$, $MgCl_2$, $NiCl_2•6H_2O$, $CoCl_2$, $FeCl_3$, NaCl, KCl, $CuCl_2$, $MnCl_2$)

in MilliQ water. For each metal study, take Zn^{2+} as an example, 5 µL of a 0.1 M Zn^{2+} stock solution was added to 50 µL of a 2 mM liposome containing 10% of **1** obtained from the procedure above (final concentration for Zn^{2+} ≈ 10 mM). Fluorescence intensities were taken after 40 min incubation time with the same fluorescence detection method as titration. Studies with other ions were done in the same manner. A control experiment was also run by adding 5 µL MilliQ water to 50 µL of the same liposome to test the dilution effect. The same liposome solution was used for one set of comparison studies using each of the described metals. When processing the data, fluorescence intensities at 620 nm were selected and the intensity decrease caused by dilution effect was again subtracted out. The whole process was repeated 3 times with different batches of liposomes, and averaged data were reported with error bars showing standard error.

Preparation of liposomes encapsulating sulforhodamine B

A 20 mM sulforhodamine B stock solution was prepared by dissolving 0.2323 g sulforhodamine B sodium salt in 20 mL MilliQ purified water. The Lipid **1** and PC stock solutions were prepared as previously described in the nile red release studies. Proper volumes of each stock solution were pipetted into a clean vial to obtain the desired percentage of each component. As an example, to make 200 µL of a 2 mM liposome solution containing 10% of **1**, 11.3 µL PC (90%) and 8 µL lipid **1** (10%) were combined in a vial. The solvents were then removed using rotary evaporator and the resulting solid was further dried under vacuum for at least two hours to yield a lipid film. After that, the lipid film was hydrated with 200 µL of the 20 mM sulforhodamine B stock solution at 50 °C for 3 sets of 10 mins with vortexing after each set. 10 freeze-thaw cycles were done on the resulting liposome solution with dry/ice acetone bath and 50 °C water bath. Then, the liposome solutions were extruded through a 200 nm polycarbonate membrane for 31 passes with a LiposoFast extruder (Avestin, Inc.). Finally, the unencapsulated dye was removed via a size exclusion column packed with Sephadex G-50 (pre-saturated with MilliQ water). Fractions were collected every ~1 mL and the second fraction was chosen to run further studies based on fluorescence increases observed when aliquots were treated with triton X-100.

Titrations of liposomes encapsulating sulforhodamine B with calcium chloride solutions

The calcium chloride stock solution that was used was the same as the nile red release study (0.1 M). A solution of 10% triton X-100 was prepared by dissolving 1 mL triton X-100 into 10 mL MilliQ water. A 100 µL aliquot of the liposome solution prepared through the procedure above was added to a sub-micro quartz cuvette. The calcium chloride stock solution was added in 1.0 µL aliquots directly into the cuvette for each measurement in the titration (increment ~ 1.0 mM) and the fluorescence intensity was then measured using an average of 3 scans. (excitation wavelength = 550 nm, excitation slit = 7.5 nm, emission slit = 5.0 nm). After adding 20 mM Ca^{2+}, 2 uL 10% of triton X-100 was added to trigger complete release. When processing the data, fluorescence intensities at 585 nm were selected and fluorescence increases were reported as a percentage of the fluorescence after triton X-100 treatment for each sample. Experiments were run at least 3 times each with different batches of liposomes, and averaged data were reported with error bars showing standard error.

STEM imaging of liposome samples

2 mM Liposomes consisting of only PC or 10% lipid **1** and 90% PC were prepared as previously described. As an example, to make 250 µL 10% liposomes, 14.1 µL PC (90%) and 10 µL lipid **1** were pipetted into a vial. After preparing the lipid films, 250 µL MilliQ water was added to hydrate, followed by 10 freeze-thaw cycles and extrusion through a 200 nm polycarbonate membrane. The formation of liposomes with desired size was confirmed by DLS. For STEM studies, a drop (5-10 µL) from each solution was immobilized onto a thin carbon film supported by a 200 mesh copper grid and then stained with a 0.5% (w/v) solution of phosphotungstic acid. After drying, the samples were stored in a desiccator overnight prior to examination. Images were collected using a Zeiss Auriga 40 microscope operating in scanning transmission (STEM) mode and a beam energy of 30keV.

Acknowledgements

We acknowledge funding for this work from the University of Tennessee. We also acknowledge Dr. John Dunlap for assistance with STEM studies.

Keywords: Drug Delivery • Liposome • Molecular Recognition • Self Assembly • Lipids

[1] a) Y. Barenholz, *J Control. Release* **2012**, *160*, 117-134; b) G. T. Noble, J. F. Stefanick, J. D. Ashley, T. Kiziltepe, B. Bilgicer, *Trends Biotechnol.* **2014**, *32*, 32-45; c) P. P. Deshpande, S. Biswas, V. P. Torchilin, *Nanomedicine* **2013**, *8*, 1509-1528.

[2] a) S. Alam, S. I. Mattern-Schain, M. D. Best, in *Comprehensive Supramolecular Chemistry Volume 2, Vol. 5* (Ed.: J. L. Atwood), Elsevier, **2017**, pp. 329-364; b) B. S. Pattni, V. V. Chupin, V. P. Torchilin, *Chem. Rev.* **2015**, *115*, 10938-10966.

[3] a) H. Ellens, J. Bentz, F. C. Szoka, *Biochemistry* **1984**, *23*, 1532-1538; b) R. M. Sawant, J. P. Hurley, S. Salmaso, A. Kale, E. Tolcheva, T. S. Levchenko, V. P. Torchilin, *Bioconjugate Chem.* **2006**, *17*, 943-949; c) A. A. Kale, V. P. Torchilin, *Bioconjugate Chem.* **2007**, *18*, 363-370; d) X. Guo, L. Gagne, H. G. Chen, F. C. Szoka, *J. Liposome Res.* **2014**, *24*, 90-98; e) Y. Liu, L. L. Li, G. B. Qi, X. G. Chen, H. Wang, *Biomaterials* **2014**, *35*, 3406-3415; f) W. Viricel, A. Mbarek, J. Leblond, *Angew. Chem., Int. Edit.* **2015**, *54*, 12743-12747; g) A. A. Yaroslavov, A. V. Sybachin, O. V. Zaborova, V. A. Migulin, V. V. Samoshin, M. Ballauff, E. Kesselman, J. Schmidt, Y. Talmon, F. M. Menger, *Nanoscale* **2015**, *7*, 1635-1641.

[4] a) N. L. Abbott, C. M. Jewell, M. E. Hays, Y. Kondo, D. M. Lynn, *J. Am. Chem. Soc.* **2005**, *127*, 11576-11577; b) W. Ong, Y. M. Yang, A. C. Cruciano, R. L. McCarley, *J. Am. Chem. Soc.* **2008**, *130*, 14739-14744; c) I. Y. Kim, Y. S. Kang, D. S. Lee, H. J. Park, E. K. Choi, Y. K. Oh, H. J. Son, J. S. Kim, *J. Control. Release* **2009**, *140*, 55-60; d) D. Correia-Ledo, A. A. Arnold, J. Mauzeroll, *J. Am. Chem. Soc.* **2010**, *132*, 15120-15123.

[5] a) C. Foged, H. M. Nielsen, S. Frokjaer, *Int. J. Pharmaceutics* **2007**, *331*, 160-166; b) A. I. Elegbede, J. Banerjee, A. J. Hanson, S. Tobwala, B. Ganguli, R. Y. Wang, X. N. Lu, D. K. Srivastava, S. Mallik, *J. Am. Chem. Soc.* **2008**, *130*, 10633-10642; c) L. Linderoth, G. H. Peters, R. Madsen, T. L. Andresen, *Angew. Chem., Int. Edit.* **2009**, *48*, 1823-1826; d) D. S. Guo, K. Wang, Y. X. Wang, Y. Liu, *J. Am. Chem. Soc.* **2012**, *134*, 10244-10250; e) L. Zhu, P. Kate, V. P. Torchilin, *ACS Nano* **2012**, *6*, 3491-3498; f) Y. Wan, J. F. Han, G. R. Fan, Z. R. Zhang, T. Gong, X. Sun, *Biomaterials* **2013**, *34*, 3020-3030; g) S. Thamphiwatana, W. W. Gao, D. Pornpattananangkul, Q. Z. Zhang, V. Fu, J. Y. Li, J. M. Li, M. Obonyo, L. F. Zhang, *J. Mater. Chem. B* **2014**, *2*, 8201-8207.

[6] a) N. J. Wymer, O. V. Gerasimov, D. H. Thompson, *Bioconjugate Chem.* **1998**, *9*, 305-308; b) Z. Y. Zhang, B. D. Smith, *Bioconjugate Chem.* **1999**, *10*, 1150-1152; c) Z. G. Li, Y. Q. Wan, A. G. Kutateladze, *Langmuir* **2003**, *19*, 6381-6391; d) T. Nagasaki, A. Taniguchi, S. Tamagaki, *Bioconjugate Chem.* **2003**, *14*, 513-516; e) R. N. Ezhov, V. V. Rozhkov, J. R. R. Majjigapu, A. G. Kutateladze, *J. Sulfur Chem.* **2008**, *29*, 389-400; f) J. M. Dong, Z. Q. Xun, Y. Zeng, T. J. Yu, Y. B. Han, J. P. Chen, Y. Y. Li, G. Q. Yang, Y. Li, *Chem. Eur. J.* **2013**, *19*, 7931-7936; g) A. M. Bayer, S. Alam, S. I. Mattern-Schain, M. D. Best, *Chem. Eur. J.* **2014**, *20*, 3350-3357; h) S. Alam, D. S. Alves, S. A.

Whitehead, A. M. Bayer, C. D. McNitt, V. V. Popik, F. N. Barrera, M. D. Best, *Bioconjugate Chem.* **2015**, *26*, 1021-1031; i) J. Sine, C. Urban, D. Thayer, H. Charron, N. Valim, D. B. Tata, R. Schiff, R. Blumenthal, A. Joshi, A. Puri, *Int. J. Nanomed.* **2015**, *10*, 125-145; j) D. D. Luo, K. A. Carter, A. Razi, J. M. Geng, S. Shao, D. Giraldo, U. Sunar, J. Ortega, J. F. Lovell, *Biomaterials* **2016**, *75*, 193-202; k) Y. W. Sun, Y. Y. Ji, H. Y. Yu, D. Wang, M. W. Cao, J. Q. Wang, *RSC Adv.* **2016**, *6*, 81245-81249.

[7] a) Y. Negishi, D. Omata, H. Iijima, Y. Takabayashi, K. Suzuki, Y. Endo, R. Suzuki, K. Maruyama, M. Nomizu, Y. Aramaki, *Mol. Pharm.* **2010**, *7*, 217-226; b) P. Li, Y. Y. Zheng, H. T. Ran, J. X. Tan, Y. J. Lin, Q. X. Zhang, J. L. Ren, Z. G. Wang, *J. Control. Rel.* **2012**, *162*, 349-354; c) M. van Elk, R. Deckers, C. Oerlemans, Y. Shi, G. Storm, T. Vermonden, W. E. Hennink, *Biomacromolecules* **2014**, *15*, 1002-1009; d) X. L. Liang, J. Gao, L. D. Jiang, J. W. Luo, L. J. Jing, X. D. Li, Y. S. Jin, Z. F. Dai, *ACS Nano* **2015**, *9*, 1280-1293.

[8] a) K. J. Chen, H. F. Liang, H. L. Chen, Y. C. Wang, P. Y. Cheng, H. L. Liu, Y. N. Xia, H. W. Sung, *ACS Nano* **2013**, *7*, 438-446; b) Y. J. Jing, H. D. Trefna, M. Persson, S. Svedhem, *Biochim. Biophys. Acta* **2015**, *1848*, 1417-1423; c) L. Li, T. L. M. ten Hagen, D. Schipper, T. M. Wijnberg, G. C. van Rhoon, A. M. M. Eggermont, L. H. Lindner, G. A. Koning, *J. Control. Release* **2010**, *143*, 274-279; d) A. Lopez-Noriega, E. Ruiz-Hernandez, E. Quinlan, G. Storm, W. E. Hennink, F. J. O'Brien, *J. Control. Release.* **2014**, *187*, 158-166; e) T. Lu, W. J. M. Lokerse, A. L. B. Seynhaeve, G. A. Koning, T. L. M. ten Hagen, *J. Control. Release.* **2015**, *220*, 425-437; f) A. Ranjan, G. C. Jacobs, D. L. Woods, A. H. Negussie, A. Partanen, P. S. Yarmolenko, C. E. Gacchina, K. V. Sharma, V. Frenkel, B. J. Wood, M. R. Dreher, *J. Control. Release* **2012**, *158*, 487-494; g) M. B. Yatvin, J. N. Weinstein, W. H. Dennis, R. Blumenthal, *Science* **1978**, *202*, 1290-1293.

[9] a) R. J. Gillies, Z. Liu, Z. Bhujwalla, *Am. J. Physiol.* **1994**, *267*, C195-C203; b) R. van Sluis, Z. M. Bhujwalla, N. Raghunand, P. Ballesteros, J. Alvarez, S. Cerdan, J. P. Galons, R. J. Gillies, *Magn. Res. Med.* **1999**, *41*, 743-750.

[10] S. Orrenius, V. Gogvadze, B. Zhivotovsky, *Biochem. Biophys. Res. Commun.* **2015**, *460*, 72-81.

[11] M. K. Tu, J. B. Levin, A. M. Hamilton, L. N. Borodinsky, *Cell Calcium* **2016**, *59*, 91-97.

[12] a) A. Ghosh, M. E. Greenberg, *Science* **1995**, *268*, 239-247; b) C. Grienberger, A. Konnerth, *Neuron* **2012**, *73*, 862-885.

[13] E. M. Gallo, K. Cante-Barrett, G. R. Crabtree, *Nat. Immunol.* **2006**, *7*, 25-32.

[14] M. Peacock, *Clin. J. Am. Soc. Nephrlo.* **2010**, *5 Suppl 1*, S23-30.

[15] W. G. Robertson, R. W. Marshall, M. Walser, *CRC Crit. Rev. Clin. Lab. Sci.* **1979**, *11*, 271-304.

[16] N. Prevarskaya, R. Skryma, Y. Shuba, *Nat. Rev. Cancer* **2011**, *11*, 609-618.

[17] D. E. Clapham, *Cell* **2007**, *131*, 1047-1058.

[18] a) G. E. Stutzmann, M. P. Mattson, *Pharmacol. Rev.* **2011**, *63*, 700-727; b) A. Verkhratsky, *Physiol. Rev.* **2005**, *85*, 201-279.

[19] I. Bezprozvanny, M. P. Mattson, *Trends Neurosci.* **2008**, *31*, 454-463.

[20] a) Kruman, II, W. A. Pedersen, J. E. Springer, M. P. Mattson, *Exp.Neurol.* **1999**, *160*, 28-39; b) S. S. Leal, C. M. Gomes, *Front. Cell. Neurosci.* **2015**, *9*.

[21] a) D. S. T. Ong, T.-W. Mu, A. E. Palmer, J. W. Kelly, *Nat. Chem. Biol.* **2010**, *6*, 424-432; b) E. B. Vitner, F. M. Platt, A. H. Futerman, *J. Biol. Chem.* **2010**, *285*, 20423-20427.

[22] J. F. MacDonald, Z. G. Xiong, M. F. Jackson, *Trends Neurosci.* **2006**, *29*, 75-81.

[23] M. Brochet, O. Billker, *Molec. Microbiol.* **2016**, *100*, 397-408.

[24] P. Ward, L. Equinet, J. Packer, C. Doerig, *BMC Genomics* **2004**, *5*.

[25] S. Glushakova, V. Lizunov, P. S. Blank, K. Melikov, G. Humphrey, J. Zimmerberg, *Malaria J.* **2013**, *12*, 12:41.

[26] a) K. Tanabe, R. B. Mikkelsen, D. F. H. Wallach, *J. Cell Biol.* **1982**, *93*, 680-684; b) J. Krungkrai, Y. Yuthavong, *Molec. Biochem. Parasitol.* **1983**, *7*, 227-235.

[27] a) M. Wasserman, J. Chaparro, *Parasitol. Res.* **1996**, *82*, 102-107; b) S. Garg, S. Agarwal, S. Kumar, S. S. Yazdani, C. E. Chitnis, S. Singh, *Nat. Commun.* **2013**, *4*.

[28] a) P. Sundaramoorthy, J. J. Sim, Y.-S. Jang, S. K. Mishra, K.-Y. Jeong, P. Mander, O. B. Chul, W.-S. Shim, S. H. Oh, K.-Y. Nam, H. M. Kim, *PLoS One* **2015**, *10*, e0116984; b) N. Prevarskaya, R. Skryma, Y. Shuba, *Exp. Opin. Ther. Targets* **2013**, *17*, 225-241.

[29] K. T. Chan, D. A. Bennin, A. Huttenlocher, *J. Biol. Chem.* **2010**, *285*, 11418-11426.

[30] W. Viricel, A. Mbarek, J. Leblond, *Angew. Chem., Int. Edit.* **2015**, *54*, 12743-12747.

[31] A. J. Plaunt, K. M. Harmatys, K. A. Hendrie, A. J. Musso, B. D. Smith, *RSC Adv.* **2014**, *4*, 57983-57990.

[32] a) G. Grynkiewicz, M. Poenie, R. Y. Tsien, *J. Biol. Chem.* **1985**, *260*, 3440-3450; b) R. Y. Tsien, *Annu. Rev. Neurosci.* **1989**, *12*, 227-253; c) S. Sumalekshmy, C. J. Fahrni, *Chem. Mater.* **2011**, *23*, 483-500.

[33] E. V. van den Brink-van der Laan, J. A. Killian, B. de Kruijff, *Biochim. Biophys. Acta* **2004**, *1666*, 275-288.

[34] a) X. L. Liang, X. L. Yue, Z. F. Dai, J. Kikuchi, *Chem. Commun.* **2011**, *47*, 4751-4753; b) A. M. Bayer, S. Alam, S. I. Mattern-Schain, M. D. Best, *Chem. Eur. J.* **2014**, *20*, 3350-3357.

[35] D. Papahadjopoulos, S. Nir, N. Duzgunes, *J Bioenerg. Biomembr.* **1990**, *22*, 157-179.

10.1002/chem.201705810

WILEY-VCH

FULL PAPER

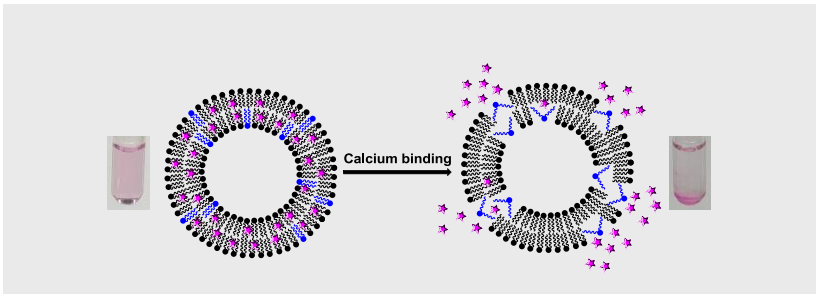

J. Lou, A.J. Carr, A.J. Watson, S.I. Mattern-Schain and M.D. Best

Page No. – Page No.

Calcium-Responsive Liposomes via a Synthetic Lipid Switch